

The presence of a (1 × 1) oxygen overlayer on ZnO(0001) surfaces and at Schottky interfaces

This article has been downloaded from IOPscience. Please scroll down to see the full text article.

2012 J. Phys.: Condens. Matter 24 095007

(<http://iopscience.iop.org/0953-8984/24/9/095007>)

View [the table of contents for this issue](#), or go to the [journal homepage](#) for more

Download details:

IP Address: 141.211.173.82

The article was downloaded on 26/06/2013 at 16:05

Please note that [terms and conditions apply](#).

The presence of a (1 × 1) oxygen overlayer on ZnO(0001) surfaces and at Schottky interfaces

Christian M Schlepütz^{1,5}, Yongsoo Yang¹, Naji S Hussein¹, Robert Heinhold^{2,3}, Hyung-Suk Kim^{2,3}, Martin W Allen^{2,3}, Steven M Durbin^{2,4} and Roy Clarke¹

¹ Department of Physics, University of Michigan, Ann Arbor, MI 48109, USA

² MacDiarmid Institute for Advanced Materials and Nanotechnology, New Zealand

³ Department of Electrical and Computer Engineering, University of Canterbury, Christchurch 8140, New Zealand

⁴ Department of Electrical Engineering and Department of Physics, University at Buffalo, Buffalo, NY 14260, USA

E-mail: cschlep@aps.anl.gov

Received 25 October 2011, in final form 12 January 2012

Published 3 February 2012

Online at stacks.iop.org/JPhysCM/24/095007

Abstract

The atomic surface and interface structures of uncoated and metal-coated epi-polished ZnO(0001) Zn-polar wafers were investigated via surface x-ray diffraction. All uncoated samples showed the presence of a fully occupied (1 × 1) overlayer of oxygen atoms located at the on-top position above the terminating Zn atom, a structure predicted to be unstable by several density functional theory calculations. The same oxygen overlayer was clearly seen at the interface of ZnO with both elemental and oxidized metal Schottky contact layers. No significant atomic relaxations were observed at surfaces and interfaces processed under typical device fabrication conditions.

(Some figures may appear in colour only in the online journal)

1. Introduction

ZnO has many important technological applications in fields as diverse as catalysis, gas sensing, corrosion prevention, and optoelectronics [1]. A precise knowledge of the structural properties of the surfaces and interfaces involved in these applications is a prerequisite for their control and optimization. However, despite a large number of experimental and theoretical studies, the respective structures of ZnO surfaces and interfaces remain a topic of intensive debate, with many alternative structures already described [1–9]. This lack of consensus arises primarily from the competition of various surface-stabilization mechanisms and a host of different preparation procedures and ambient conditions, resulting in a complex phase diagram [7–9].

⁵ Present address: Argonne National Laboratory, Argonne, IL 60439, USA.

We report on a systematic study of the atomic structure of uncoated ZnO surfaces and metal Schottky contacts to ZnO prepared under typical device fabrication conditions. Schottky contacts are important building blocks in many electronic devices, and an understanding of their interface structure is crucial, since electronic and structural properties are usually strongly correlated. This is particularly true for semiconductors characterized by highly ionic bonding (e.g., ZnO), in which small atomic displacements can potentially result in large changes in electronic behavior.

2. Methods

Single-crystal ZnO(0001) wafers were hydrothermally grown along the +*c*-axis by Tokyo Denpa Co., Ltd, and epi-polished to low miscut angles (<0.1°) [10]. For measurements on uncoated surfaces, samples 1–3 were ultrasonically cleaned

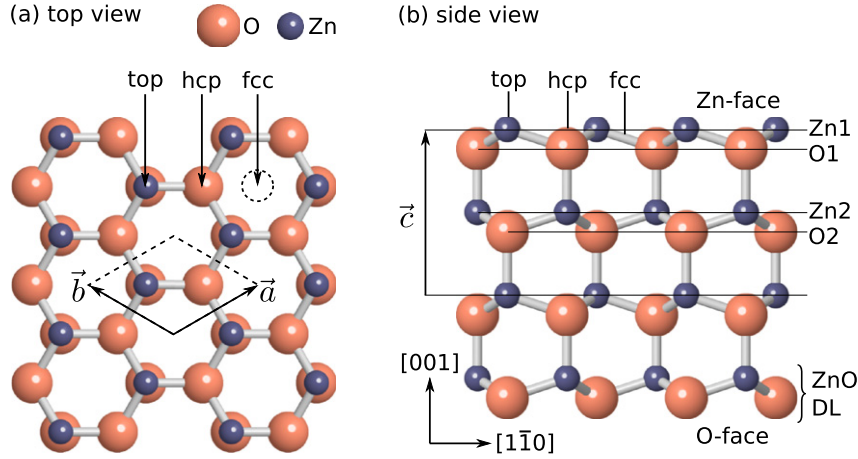


Figure 1. Atomic structure of a bulk-like ZnO(0001) surface. (a) Top view with the surface unit cell. (b) Side view along the $[110]$ direction. Note the presence of two ZnO double layers (DLs) within the unit-cell height c . Also indicated are the three high-symmetry positions in the crystal unit cell at the on-top (top), hcp hollow (hcp) and fcc hollow (fcc) sites.

Table 1. List of investigated samples.

Sample	1	2	3	4	5	6	7
Cap layer	—	—	—	Au	Au	IrO _x	IrO _x
Thickness (nm)	—	—	—	40	25	40	25
Beamline	SLS	SLS	SLS	SLS	APS	SLS	APS
Total SF	1180	2082	2446	1891	997	2030	596
Averaged SF	536	699	629	651	606	683	416
σ_{sym} (%)	5.3	8.7	8.6	8.5	8.5	9.7	6.4

for 3–4 min in acetone and rinsed using isopropyl alcohol (IPA), dried in N₂, and subsequently exposed to air. Polycrystalline Schottky contacts were deposited on other samples after the same cleaning procedure, either as plain gold by thermal evaporation (samples 4, 5) or in the form of non-stoichiometric iridium oxide (IrO_x) layers by eclipse pulsed laser deposition in an oxygen ambient (samples 6, 7). The latter method has been shown to produce high-quality Schottky contacts to ZnO [11].

Surface x-ray diffraction (SXRD) can access the buried interface structures of the Schottky contacts non-destructively, and it provides picometer accuracy for determining atomic positions. Experiments were carried out on the Materials Science beamline X04SA at the Swiss Light Source (SLS) and on the GeoSoilEnviroCARS beamline, 13-BMC, at the Advanced Photon Source (APS), using a PILATUS 100K pixel detector for fast and reliable data acquisition [12, 13].

For each sample, at least eight symmetrically inequivalent ($p6mm$) plus several equivalent crystal truncation rods (CTRs) were recorded, typically resulting in 400–700 averaged structure factors (SFs) per data set and systematic errors of 5–10% between symmetry equivalents (see table 1). The measured SFs were fitted using a specialized module to model SXRD data for the genetic algorithm refinement program GenX [14]. Using differential evolution algorithms, GenX efficiently avoids becoming trapped in local minima. All fits were repeated at least ten times with random parameter initializations to verify the reproducibility and uniqueness of

a solution. To give the low-intensity regions of the CTRs a similar weight in the fit to the high-intensity points close to the Bragg peaks, a logarithmic R -factor, R_{\log} , was employed for the fitting figure of merit (FOM):

$$R_{\log} = \frac{\sum_i |\log_{10}(|F_i^{\text{exp}}|) - \log_{10}(|F_i^{\text{calc}}|)|}{\sum_i \log_{10}(|F_i^{\text{exp}}|)}. \quad (1)$$

All final fit results are also given in terms of the standard crystallographic R -factor:

$$R = \frac{\sum_i ||F_i^{\text{exp}}| - |F_i^{\text{calc}}||}{\sum_i |F_i^{\text{exp}}|}. \quad (2)$$

3. Results

In-plane line scans along high-symmetry directions gave no evidence for surface or interface reconstructions on any sample. The out-of-plane CTR measurements revealed a sixfold rotational symmetry of the diffraction pattern ($p6mm$), consistent with the presence of two 180°-rotated domains with local $p3m1$ symmetry separated by 1/2 unit-cell height terrace steps [2]. This agrees with atomic force microscopy (AFM) measurements on hydrothermal ZnO(0001) Zn-polar surfaces prepared in an identical manner, which have shown evidence of triangular islands and pits with 180° rotation between triangles on terraces separated by a single DL step [11].

To identify the characteristic structural features, we tested a large number of different models with varying degrees of complexity based on the bulk-like surface structure shown in figure 1. Atomic z -displacements (Δz), occupations (p_{occ}), and Debye–Waller (DW) factors of all atoms in up to four ZnO DLs were allowed to vary freely. The local $p3m1$ surface symmetry only permits atomic movements Δz along the z -direction and allows adatoms to be present in just three different positions in the unit cell: at $(x, y) = (0, 0)$ (fcc hollow), $(1/3, 2/3)$ (on top), and $(2/3, 1/3)$ (hcp hollow) [6]. In addition to testing a completely bulk-like structure, we therefore also tested various models with adatoms (both

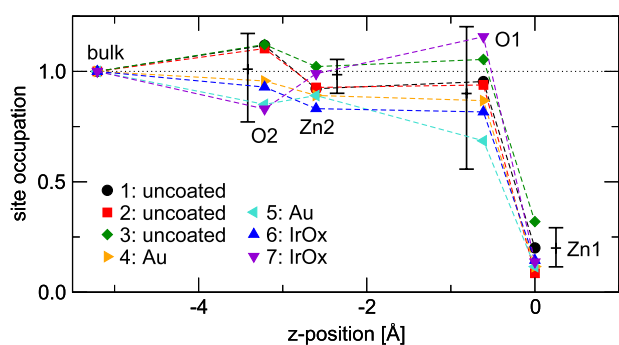


Figure 2. Fitted occupation profiles for a bulk-like model for all data sets. Average error bars of individual data points are shown next to the data.

oxygen or metal atoms) located at some or all of these allowed locations and free to move within one unit cell away from the surface.

The results of these survey fits draw a consistent picture of the chemical nature of the surfaces or interfaces across all samples, including those coated with metal Schottky layers. The occupation parameters of zinc reveal a sharp surface/interface, where only the topmost atomic layer (Zn1) is partially occupied with $p_{\text{occ}}(\text{Zn1}) < 40\%$. The oxygen (O1) occupation within the same DL is, however, close to unity, as is the zinc (Zn2) occupation in the next DL below. An example of this is seen in figure 2, which shows the fitted occupation profile for a bulk-like model without adatoms. When including the adatoms located in the high-symmetry sites on the surface in the fits, we usually observe a comparable partial occupation of oxygen adatoms above the incomplete Zn layer in the epitaxial on-top position, while the occupations in fcc and hcp hollow sites remain negligible. Consequently, we find an oxygen atom above each Zn atom in the structure, providing strong evidence for the presence of an oxygen overlayer on top of the nominally Zn-terminated surface. There are, on the other hand, no indications for the presence of any other ordered adsorbed species or, in particular, the ordering of metal atoms in those samples with metal Schottky contacts.

The partial occupation of the Zn1 layer and its associated oxygen adatoms is most likely attributable to islands and terrace steps on an otherwise atomically flat surface and is a result of averaging over more than one distinct terrace level within the coherence length of the x-rays (typically a few hundred nanometers). This scenario is consistent with AFM topography measurements on identically prepared samples [11], which show terraces extending over several hundred nm, covered with smaller islands or pits 30–200 nm in size and half a unit cell in height. As a consequence of this averaging, all atoms in the initial fits (see figure 2) represent a mixture of two or more distinct atoms in different positions with respect to the surface, which are therefore subject to chemically unequal environments. For example, a large fraction ($>60\%$) of the O1 atoms form overlayer adatoms on top of the fully occupied lower terrace level (above the Zn2 atoms), while the rest are associated with

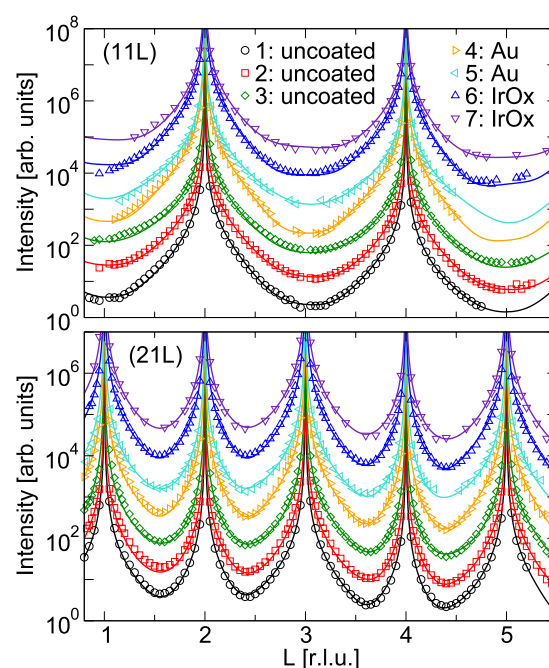


Figure 3. Measured diffraction data (open symbols) and corresponding calculated intensities (lines) based on the fitted on-top oxygen overlayer structure for two representative CTRs on all samples. Error bars are smaller than the data points and have been omitted.

fourfold-coordinated oxygen atoms within the upper terrace (below the topmost Zn1 layer).

To retrieve the structural relaxations within each individual terrace, it is therefore necessary to use a model that calculates the scattering contributions from different terrace levels separately. The total calculated scattering intensity then consists of a coherent addition of individual terrace contributions, taking into account the proper symmetry operations. These contributions are weighted by occupation factors, determined by fitting, for each terrace level. The atomic model for the structure at the individual terrace level is similar to that used in previous fits, consisting of a bulk-like Zn-terminated surface with possible adatoms at the high-symmetry on-top, fcc hollow, and hcp hollow sites. Only the adatom occupations are allowed to vary, as all the other occupation parameters are determined through the terrace occupations. Displacement and DW factors were fitted down to the second DL, including overlayer adatoms.

Regarding the presence and nature of the oxygen overlayer, the terrace model confirmed the initial results. Most importantly, we found no indications for structural differences between the uncoated and metal-covered samples. This is qualitatively evident from their exceedingly similar CTR shapes (see figure 3), as large changes in the measured intensities would be expected if either an ordering of the relatively heavy metal atoms or a significant rearrangement of zinc or oxygen atoms at the interface did occur. When fitting the oxygen occupations of all high-symmetry adatoms simultaneously, the coverages for the on-top atoms were consistently close to unity, while the fcc and bcc hollow sites showed significantly smaller occupations. Alternatively,

Table 2. Final fit results on all samples. R_{\log} and R are given in per cent (%); z -displacements, Δz , have units of picometers (pm). Uncertainties in the last digits are shown in parentheses, i.e., 0.33(73) reads 0.33 ± 0.73 .

Sample	1	2	3	4	5	6	7
R_{\log}	3.90	1.64	1.56	1.71	1.49	2.07	1.68
R	5.88	6.78	7.16	7.53	4.71	8.23	4.49
$p_{\text{occ}}(\text{O}_{\text{OL}})$	1.00(12)	1.00(30)	1.00(41)	1.00(21)	0.89(30)	1.00(26)	0.92(39)
$\Delta z(\text{O}_{\text{OL}})$	11(11)	18(20)	4(30)	26(12)	-13(16)	18(20)	-1(18)
$\Delta z(\text{Zn1})$	0.40(80)	-0.90(71)	-0.89(88)	0.76(94)	0.33(73)	1.27(1.16)	0.22(80)
$\Delta z(\text{O1})$	-9.7(3.5)	-2.7(3.3)	-4.3(5.9)	-5.0(4.3)	-0.1(4.6)	-3.1(5.0)	-7.6(7.2)
$\Delta z(\text{Zn2})$	-0.50(67)	-0.38(62)	-0.99(92)	-0.39(70)	-0.31(1.01)	-0.45(81)	-0.34(80)
$\Delta z(\text{O2})$	-5.4(4.2)	-1.4(3.3)	-3.7(5.0)	-0.6(4.8)	-4.9(5.2)	-1.1(6.2)	-3.1(5.5)

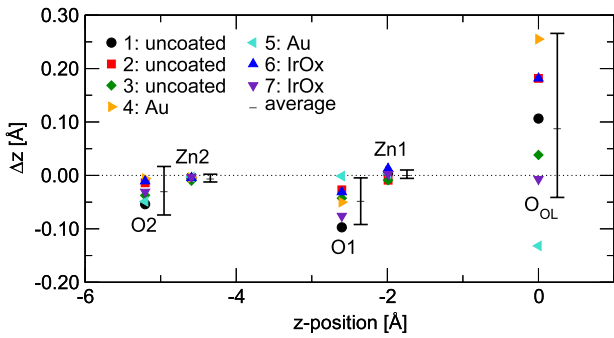


Figure 4. Fitted z -displacements Δz for all samples. Average displacement values and averaged error bars are shown to the right of the data points of individual samples. Refer to table 2 for a complete list of parameter values and uncertainties.

when allowing oxygen to be present at only one of the three sites, the lowest FOM on all samples was always achieved with the overlayer atom in the on-top position. Finally, oxygen adatoms always produced better fits than other adatom species—in particular, any of the metals used to produce the Schottky contacts.

On the basis of this evidence, the on-top oxygen overlayer was accepted as the best description of the surface structure. Figure 3 shows the excellent agreement between measured diffraction data and simulated CTR profiles. The corresponding final FOM values and fit parameters are summarized in table 2. All ten randomly initialized fits for each sample converged to the identical solution. The occupation of the overlayer atom, O_{OL} , was consistently found to be unity within the error bars, resulting in a fully covered (1×1) surface structure. The DW factors within the topmost ZnO DLs always gave values close to those reported for bulk crystals [15], and manually modifying them had no significant influence on the optimized values of any other parameters. For the overlayer oxygen atoms, the fitted DW factors were on average approximately ten times higher than for those in the bulk.

The fitted z -displacements are plotted in figure 4. There are no detectable atomic movements of the Zn atoms, while the O1 and O2 atoms seem to relax inwards slightly on average. However, the observed displacements are small (<10 pm; see table 2) and the sample-to-sample fluctuations of the results are comparable to the observed effect. The

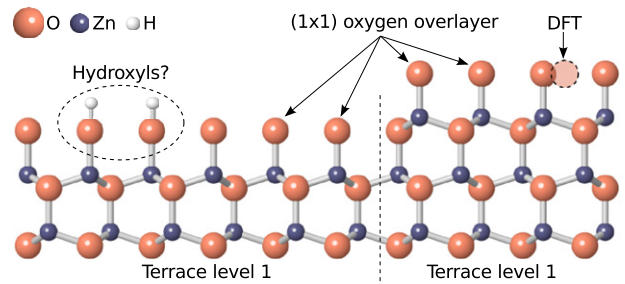


Figure 5. Atomic model of the structure giving the best fit to the experimental data, shown in the presence of a terrace step. A (1×1) oxygen overlayer in the on-top position above the last zinc atom covers the entire surface, and is most likely associated with hydroxyl groups in the case of the uncoated surfaces. Also indicated is the most stable oxygen adsorption site predicted by DFT calculations, which is at the fcc hollow site [7–9].

error bars of individual displacement values, defined through a 5% increase of the FOM value [14], are of similar magnitude. The average sizes of error bars and average displacement values are shown to the right of the data points in figure 4. For the O_{OL} atom, most samples show an outward relaxation, but again, the displacements are comparable to the sample-to-sample variations and the individual error bars. The values are also compatible with zero displacements, given their individual uncertainties as listed in table 2 (sample 4 seems to be something of an outlier, but remains within statistically reasonable limits). In conclusion, we do not observe any significant displacements larger than the experimental uncertainties. This is qualitatively consistent with the very symmetric CTR shapes shown in figure 3, as considerable asymmetries in the CTRs indicate strong relaxations.

4. Discussion and conclusions

The structural results are summarized in the atomic model shown in figure 5. The observed (1×1) oxygen overlayer on the uncoated Zn-polar ZnO surface is most likely associated with a fully hydroxylated surface, as has been observed by x-ray photoemission spectroscopy (XPS) [16–18]. The presence of hydroxyl (OH) groups, instead of only the observed oxygen atoms, is consistent with the SXRD data, since SXRD lacks sufficient sensitivity for detecting the

single electron belonging to the hydrogen atoms of the OH groups. Previous XPS measurements on the same epi-polished hydrothermal ZnO material indicate a stable OH coverage of at least one monolayer (ML) on the Zn-polar face [18]. The bonding of these hydroxyl groups on the Zn-polar face appears to be very stable, with the XPS signal associated with surface OH bonds remaining clearly visible upon heating of samples in vacuum up to approximately 600 °C. Typically, several sputtering and annealing cycles are necessary to completely remove all traces of the OH coverage [19].

Interestingly, the ordered (1 × 1) oxygen layer remains intact when the surfaces are covered with plain or oxidized metal Schottky contacts. The presence of oxygen at the interface is consistent with *ab initio* calculations of the adsorption of Cu atoms on polar ZnO surfaces and the role of chemical bonding at metal–ZnO interfaces, which indicate that a direct metal–zinc bonding is unfavorable and associated with Ohmic rather than the experimentally observed Schottky contact behavior [20–22]. Whether metal adsorption occurs on top of the surface OH groups or by replacing the H atoms remains unclear from the experimental results, as the detection of hydrogen at buried interfaces is extremely challenging.

From a theoretical standpoint, the formation of a (1 × 1) oxygen or hydroxyl overlayer is not well understood, as such an arrangement violates the electron counting rule and has been predicted to be thermodynamically unfavorable by density functional theory (DFT) [8, 9, 20, 23, 24]. Furthermore, this fully occupied overlayer does not appear in any of the calculated phase diagrams for ZnO, which predict no stable phases with greater than 1/2 ML OH coverage and OH adsorption at fcc hollow rather than on-top sites [7–9] (see figure 5). Our experimental results therefore indicate that alternative stabilization mechanisms that differ from those seen in DFT results may play an important role at surfaces prepared under typical device fabrication conditions.

In conclusion, SXRD has shown that the atomic structure of uncoated and metal-covered epi-polished ZnO (0001) Zn-polar surfaces prepared under typical device fabrication conditions has a bulk-like termination with no significant atomic relaxations. Most interestingly, a stable (1 × 1) overlayer of oxygen atoms on top of the terminating zinc atoms was observed, consistent with XPS measurements but at odds with DFT calculations. At uncoated surfaces, this (1 × 1) oxygen overlayer is most likely associated with the presence of hydroxyl (OH) groups. Significantly, no structural changes occur and the (1 × 1) oxygen overlayer remains in place following the fabrication of both plain and oxidized metal Schottky contacts.

Acknowledgments

The authors thank Matts Björck for supporting *GenX* and making it freely available [25]. Excellent beamline support by P R Willmott, P J Eng, and the staff of the SLS and

APS is gratefully acknowledged. Use of the Advanced Photon Source, an Office of Science User Facility operated for the US Department of Energy (DOE) Office of Science by Argonne National Laboratory, was supported by the US DOE under Contract No. DE-AC02-06CH11357. This work was supported by the New Zealand Marsden Fund (Contract No. UOC0909), and the US Department of Energy (Contract No. DE-FG02-06ER46273, PI: RC).

References

- [1] Wöll C 2007 *Prog. Surf. Sci.* **82** 55
- [2] Jedrecy N, Sauvage-Simkin M and Pinchaux R 2000 *Appl. Surf. Sci.* **162/163** 69–73
- [3] Wander A, Schedin F, Steadman P, Norris A, McGrath R, Turner T, Thornton G and Harrison N 2001 *Phys. Rev. Lett.* **86** 3811–4
- [4] Dulub O, Diebold U and Kresse G 2003 *Phys. Rev. Lett.* **90** 016102
- [5] King S T, Parihar S S, Pradhan K, Johnson-Steigelman H T and Lyman P F 2008 *Surf. Sci. Lett.* **602** L131–4
- [6] Valtiner M, Torrelles X, Pareek A, Borodin S, Gies H and Grundmeier G 2010 *J. Phys. Chem. C* **114** 15440–7
- [7] Kresse G, Dulub O and Diebold U 2003 *Phys. Rev. B* **68** 245409
- [8] Valtiner M, Todorova M, Grundmeier G and Neugebauer J 2009 *Phys. Rev. Lett.* **103** 065502
- [9] Valtiner M, Todorova M and Neugebauer J 2010 *Phys. Rev. B* **82** 165418
- [10] Ohshima E 2004 *J. Cryst. Growth* **260** 166–70
- [11] Allen M W, Mendelsberg R J, Reeves R J and Durbin S M 2009 *Appl. Phys. Lett.* **94** 103508
- [12] Schlepütz C M, Herger R, Willmott P R, Patterson B D, Bunk O, Brönnimann C, Henrich B, Hülsen G and Eikenberry E F 2005 *Acta Crystallogr. A* **61** 418–25
- [13] Kraft P *et al* 2009 *J. Synchrotron Radiat.* **16** 368–75
- [14] Björck M and Andersson G 2007 *J. Appl. Crystallogr.* **40** 1174–8
- [15] Sawada H, Wang R and Sleight A W 1996 *J. Solid State Chem.* **122** 148–50
- [16] Coppa B J, Fulton C C, Kiesel S M, Davis R F, Pandarinath C, Burnette J E, Nemanich R J and Smith D J 2005 *J. Appl. Phys.* **97** 103517
- [17] Valtiner M, Borodin S and Grundmeier G 2007 *Phys. Chem. Chem. Phys.* **9** 2406–12
- [18] Allen M W, Zemlyanov D Y, Waterhouse G I N, Metson J B, Veal T D, McConville C F and Durbin S M 2011 *Appl. Phys. Lett.* **98** 101906
- [19] Heinhold R, Zemlyanov D Y, Williams G T, Evans D A, Durbin S M and Allen M W 2011 Manuscript in preparation
- [20] Dong Y and Brillson L J 2007 *J. Electron. Mater.* **37** 743–8
- [21] Hegemann I, Schwaebe A and Fink K 2008 *J. Comput. Chem.* **29** 2302–10
- [22] Dai X Q, Yan H J, Wang J L, Liu Y M, Yang Z and Xie M H 2008 *J. Phys.: Condens. Matter* **20** 095002
- [23] Wander A and Harrison N M 2001 *J. Chem. Phys.* **115** 2312
- [24] Meyer B 2004 *Phys. Rev. B* **69** 045416
- [25] Björck M 2008 *GenX* homepage <http://genx.sourceforge.net>